Biomed Microdevices (2008) 10:601–610
DOI 10.1007/s10544-008-9171-x

Microneedle-based drug delivery: studies on delivery parameters and biocompatibility

Yan Wu · Yuqin Qiu · Suohui Zhang · Guangjiong Qin · Yunhua Gao

Published online: 7 March 2008

Abstract There is a significant interest in the application of microneedles in intradermal drug delivery systems. Previous studies have demonstrated that skin permeation of drugs can be increased by orders of magnitude with microneedle insertion. In this study, emphasis is placed on the development of low cost, painless intradermal microneedle systems that can enhance the percutaneous drug permeation. Microneedles of octagonal pyramidal shape with the length of 150 μm were employed, and the capabilities of skin permeation enhancement under different delivery conditions were examined. The delivery parameters taken into account included the insertion time and the area of insertion. It was found that when solid microneedle arrays of 150 μm in length were pierced into human dermatomed skin for 5 to 60 s, microconduits with the depth of 50 to 80 μm were created to facilitate the percutaneous permeation of drugs. In percutaneous tests, it was demonstrated that the permeability coefficient of calcein (MW=622.55) was significantly increased by 10^4 to 10^5 times compared to that on intact skin. In terms of biocompatibility, biological evaluation indicated a broad spectrum of safety for the microneedle system. These results suggest that the octagonal pyramidal microneedles can be an effective tool in developing novel intradermal drug delivery system.

Y. Wu · Y. Qiu · S. Zhang · G. Qin · Y. Gao (✉)
Laboratory of Organic Optoelectronic Functional Materials and Molecular Engineering, Technical Institute of Physics and Chemistry, Chinese Academy of Sciences, Beijing 100080, People's Republic of China
e-mail: yhgao@mail.ipc.ac.cn

Y. Wu · Y. Qiu · S. Zhang · G. Qin
Graduate University, Chinese Academy of Sciences, Beijing 100049, People's Republic of China

Keywords Microneedle · BioMEMS · Intradermal drug delivery · *In vitro* · Biocompatibility

1 Introduction

In the delivery of pharmaceuticals, transdermal drug delivery has been considered as a patient-friendly approach full of promise, since it overcomes the problems such as the hepatic first pass metabolism and poor bioavailability associated with oral delivery of biologics, and the injection pain of hypodermic needles. However, the stratum corneum constitutes a major barrier for the permeation of pharmaceuticals. To date, various methods have been explored to promote transfer of therapeutic drugs through the skin. Compared with other approaches such as electroporation (Prausnitz 1999), ultrasonic enhancement (Mitragotri and Kost 2004), or chemical enhancers (Williams and Barry 2004), which rely on physical or chemical means to decrease the permeation barrier of the stratum corneum, microneedles have a significant advantage by forming microconduits in the stratum corneum. Their sharp tips and short length reduce the odds of encountering a nerve. Thus, microneedles provide a minimally invasive means to transport molecules with various physical and chemical properties into the intradermal layer of skin. As a simple mechanical device, the microneedle drug delivery system is expected to be less invasive, less expensive and easy to use.

Over the past few years, silicon microneedles with different shapes have been fabricated, either by wet etching or dry etching technologies. Although dry etching is capable of forming microneedles of various shapes through appropriate mask and process, it is much more expensive and requires considerable effort in process development for reproducible results. In comparison, wet etching process

depends strongly on crystal planes' orientation to fabricate microneedles with a predefined shape. It's less expensive and can often lead to a controllable process, facilitating batch fabrication of wafers for low cost scalable process. Our group has developed a fabrication method to form microneedles with an octagonal pyramid shape (Xu and Gao 2003). The formed microneedles show excellent mechanical properties; they can withstand multiple skin insertion without any breakage. A later study reported that the force to break such a needle depended on the needle size and shear height (Wilke et al. 2005). Tested microneedles (179, 219, 279 μm long) have shear strengths of $(11\pm4)\times10^6$ Pa, larger than the theoretical pressure required to pierce human skin as 3.183×10^6 Pa (Aggarwal and Johnston 2004). Morrissey et al. (2005) investigated the mechanical properties of the octagonal pyramidal microneedles, reaching the conclusion that silicon microneedles were robust enough for transdermal drug delivery. Those wet-etched microneedles have already been employed as silicon-based arrays of microneedle electrodes in cancer therapy (Morrissey et al. 2004). However, there has not been any experimental data from the study of these microneedles incorporated into an intradermal microneedle drug delivery system. We believe this is the first report of a systematic experimental study of intradermal drug delivery system based on these novel microneedles.

The thicknesses of stratum corneum, viable epidermis and dermis of typical human skin are 10–20μm, 50–100μm and 1–2 mm, respectively (Prausnitz et al. 2004). Although it was reported that microneedles minimized the possibility of touching nerves (Prausnitz 2004; Martanto et al. 2004), the needle length is still limited to reach viable epidermis only to avoid pain for a microneedle array with high density. Microneedles tested in drug delivery systems have lengths ranged in size from millimeter to micrometer (McAllister et al. 2000; Prausnitz et al. 2004; Reed and Lye 2004; Teo et al. 2006). Studies have indicated that the length of microneedles has a significant impact on the sensation caused by microneedles (Table 1); for microneedle arrays, a length of less than 200 μm has been proved to be painless. Considering the relation between microneedle length and the patients' discomfort, our goal is to develop a safe intradermal drug delivery system that would have shortest microneedles possible, that yet still provides a mechanism consistent and high transdermal permeation for drug actives.

Assessment of biocompatibility plays an important role in both occupational hazard assessment and classification as well as in medical product development. Since the application of microneedle products to skin may cause unavoidable contact of microneedles with the skin, it is fairly important to study acute dermal toxicity, primary skin irritation and biocompatibility issues from the viewpoint of safety and regulatory requirements. While there is an extensive body of data dealing with skin permeation studies, for device commercialization, data on the biocompatibility of microneedles is surprisingly limited. Mikszta et al. (2002) reported weak to very mild immune responses in humans of blunt-tipped microenhancer arrays 200 μm in length. Kotzar et al. (2002) revealed the safety of single crystal silicon as the material for implantable medical devices. Even their result indicated that silicon was safe for implantable medical devices, the processing techniques for octagonal pyramidal microneedles are different from those reported before; thereby adding a variable in the biocompatibility equation. Since the ISO 10993 battery of tests represents the minimum requirement that must be met by all of the participating nations, we use this standard for the systematic assessment of the biocompatibility of microneedle arrays.

2 Materials and methods

2.1 Materials

Calcein ($C_{30}H_{26}N_2O_{13}$, MW=622.55) was purchased from Sigma (St. Louis, MO, USA). Rhodamine B ($C_{28}H_{31}ClN_2O_3$, MW=479) was an analytical reagent, and

Table 1 The relationship between the pain caused by microneedle administration and the length of microneedles

Reference	Microneedle kind	Shape	Length (μm)	Application site	Positive control	Extent of perceived pain
Kaushik et al. 2001	Silicon microneedle array; density=400 needles/3×3 mm^2	Tip radius=1 μm	150	Arm	26 gage hypodermic needle	<3%, indistinguishable (pain rate=0.67) from a smooth surface (pain rate=0.42)
Gill et al. 2006	Single stainless steel microneedle	Tip angle=20, 55, 90°	500	Forearm	26 gage hypodermic needle	5%
		Tip angle=55°	750			10%
		Tip angle=55°	1500			35%

Carbomer 940 (Carboxyvinyl Polymer) was obtained from BF Goodrich, Germany. FITC-labeled BSA (66 kDa) was prepared by Beijing Lijingkelian Biotechnology Center.

The saturated solution of calcein was prepared by adding excess calcein to 0.1 mol/L phosphate buffered saline (PBS, pH 7.4), the mixture was shaken at 37°C overnight to obtain a saturated solution. Rhodamine B gel was prepared by dissolving rhodamine B in deionized water in the concentration of 0.042 mg/ml, then mixing the solution with 2.8% carbomer solution in the proportion of 1:1 (*w*/*w*).

Franz cells were purchased from Shanghai Kaikai Science and Technology Trade Co. Ltd., China. Each cell consists of an upper donor chamber and a lower receptor chamber with a volume of 6.5 ml. There is one sampling port for pipette removal of solution on the wall of the lower receptor chamber, and the inside diameter of the receptor chamber is 18.64 mm. A horseshoe clamp was used to secure the skin and the two compartments.

2.2 Skin donors and skin preparation

Both human and rat skin were employed in this study. Samples of human dermatomed skin with a thickness of 600 to 800 μm were obtained from the Burns Institute, 304th Clinical Department, the General Hospital of PLA, Trauma Center of Postgraduate Medical College and were free from overt pathology. The skin samples were kept frozen at -85°C and used within 3 months.

Male SD rats were obtained from Beijing Vitalriver Laboratory Animal and Technology Co. Ltd., weighing 250–300 g. Forty-eight hours before the test, rats were anesthetized by ether, and then the abdominal hair of each rat was shaved with an electric hair clipper. At the end of the administration, animals were euthanized using carbon dioxide. Full-thickness skin was removed for microscopy observation. All research protocols adhered to Guide for the Care and Use of Laboratory Animals (1996).

2.3 Microneedle arrays

A novel process was developed to get 150 μm high microneedles, leading to the fabrication of microneedles reported in published data (Xu and Gao 2003; Sasaki et al. 2007; Wilke et al. 2004; Wilke and Morrissey 2007). The finished microneedle array is presented in Fig. 1, with 121 needles perpendicular to the wafer, over an area of 4× 4 mm^2. Each microneedle has an octagonal micropyramid shape, with a base length of about 100 μm. The microneedles are 150 μm in height, having a cone angle of 38°, and the needle tip is less than 1 μm wide.

To form the microneedle intradermal drug delivery system, the array was fixed onto a supporting column of the applicator, which provided insertion force of approximately 2 N to assist the insertion. The applicator was provided by Nasheng microelectronics (Suzhou) Co. Ltd. in China.

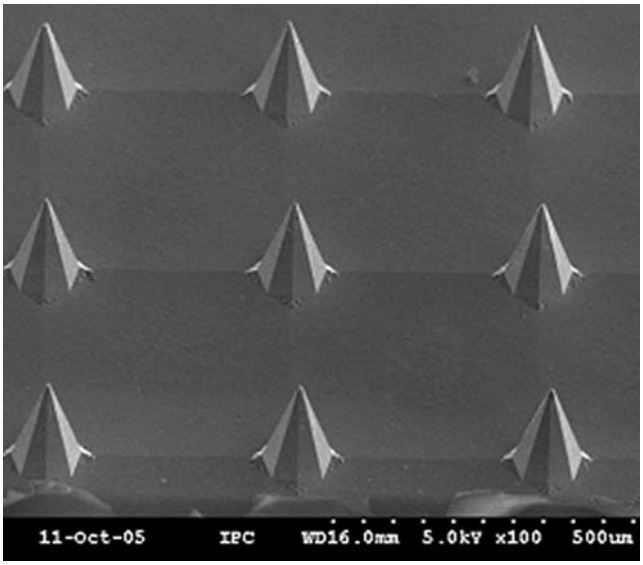

Fig. 1 The scanning electron micrograph of a section of microneedle array. The microneedle patch has microneedles of 150 μm long with a density of 484/cm^2

2.4 Microneedle–skin insertion imaging

Optical microscopic micrographs were taken, both *in vitro* and *in vivo*, to evaluate the effect of microneedle insertion.

In vitro characterization employed human dermatomed skin. Confocal laser scanning microscopy (CLSM) was employed to visualize the microconduits created in human dermatomed skin. Human dermatomed skin after insertion and removal of microneedles coated with rhodamine B gel was placed immediately upon a glass slide. At first, the stratum corneum side was examined to image the stained spots corresponding to the skin site of microneedle penetration. Then confocal laser scanning began from the stratum corneum side, at 10 μm increments through the z-axis of a ZEISS PASCAL invert confocal laser scanning microscope (LSM 510 with an attached Zeiss Axiovert 200M microscope). Optical excitations were carried out with a 543 nm HeNe laser beam and fluorescence emission was detected at 560 nm for rhodamine B. Frozen tissue sections of insertion areas were also prepared and analyzed microscopically.

To evaluate the percutaneous penetration of drugs *in vivo*, male SD rats were anaesthetized and then two protocols were followed: 10 s microneedle group (microneedle insertion for 10 s) and control group (intact skin). A piece of cotton patch saturated with FITC-BSA solution (the molar ratio of FITC to protein is 4.5) at a concentration

of 7.4 mg BSA/ml was then applied onto the skin with microneedle insertion. The cotton patch was kept in contact with the rats' skin for 1 h in both groups. Full-thickness skin was removed to observe the diffusion of fluorescent molecules by fluorescence microscopy (Olympus BX51, Olympus, Japan), with the excitation wavelength set between 470–490 nm.

2.5 *In vitro* percutaneous study through human dermatomed skin

The method of the percutaneous absorption study followed the Test Guideline 428 of Organization for Economic Cooperation and Development (2004). The experiment was performed with a system employing Franz-type glass diffusion cells. The temperature in the receptor chamber was maintained at physiological temperature of 37.0±0.1°C with an external, constant temperature circulating water bath.

After thawed in physiological saline solution, human dermatomed skin was pierced vertically by microneedles, with the insertion force of approximately 2 N provided by the applicator. The skin was mounted on a receptor chamber with the stratum corneum side facing upward into the donor chamber. The receptor and donor chambers (18.64 mm in inside diameter) were filled with PBS solution, and the receptor fluid was continuously stirred with a magnetic bar at 280 rpm to maintain homogeneity. After 1 h equilibration, the solution in the receptor chamber was replaced with fresh PBS, and the saturated calcein solution (800 μl) was applied on the skin in the donor chamber, which was then covered with a parafilm to avoid any evaporation process.

To measure percutaneous flux of calcein, samples were withdrawn through the sampling port of the diffusion cell at predetermined time intervals (10 min, 30 min, 1 h, 2 h, 4 h, 6 h and 8 h). The receptor phase was immediately replenished with equal volume of fresh PBS buffer to keep a constant volume. At least triplicate experiments were conducted for each study. Quantitative analysis of calcein was achieved by fluorescence spectroscopy using a fluorometer (F-2500, Hitachi, Japan), with the excitation and emission wavelength set at 494 and 512 nm, respectively. Similar experiments were performed with PBS buffer as the donor phase on microneedle-treated skin as a negative control.

The integrity of microneedles was examined under a stereomicroscope before and after each insertion.

2.6 Biological evaluation test

The biocompatibility study was performed in compliance with the ISO 10993 standards. All the tests were conducted at the Department of Toxicology of Peking University Health Science Center, under Institutional Animal Care and Use Committee-approved protocols. All test protocols were reviewed and approved by the Experimental Animal Ethics Committee.

The tests conducted included the bone marrow micronucleus test in mice, gene mutation in bacteria (Ames test) on four S. typhimurium strains (TA_{97}, TA_{98}, TA_{100} and TA_{102}), *in vitro* cytotoxicity test on BALB/c 3T3, *in vitro* mammalian cell gene mutation test, the maximization test and the primary skin irritation test on New Zealand white rabbits. To evaluate the safety of extractable chemicals from microneedles, the extraction was employed in these tests. The extraction was prepared by immersing silicon microneedle wafers in physiological saline at 37°C for 72 h, with a proportion of 3 cm^2 of wafer per milliliter, according to ISO 10993-12:2002 standard: "Sample Preparation and Reference Materials".

For animal studies, the route of microneedle administration was direct application of the microneedle extraction to shaved intact skin. This route of administration is standard for the assessment of local dermal irritation potential. On the day before application, hair on animals was removed from the dorsal and trunk area. On the day of dosing, but prior to application, the animals were examined for health and the skin checked for any abnormalities. No pre-existing skin irritation was observed. In maximization test, the skin sensitization reactions, including erythema and oedema, were observed and scored respectively at 24, 48 and 72 h after the removal of the test dressing. In the primary skin irritation test, irritation rate and score were calculated at 1, 24, 48 and 72 h after 4 h occlusive contact with shaved skin.

2.7 Data analysis

The percent of calcein permeated was calculated and plotted as a function of time. Steady-state skin absorption rates (J_{ss}) were determined by linear regression analysis of the amount of calcein penetrated under infinite dose conditions against time. Permeability coefficients (K_p) were calculated from the equation $K_p=J_{ss}/C_0$, where C_0 was the concentration of the agent applied to the skin surface. The diffusional lag-time was estimated from the *x*-axis intercept of the amount penetrated under infinite dose conditions against time during steady-state conditions. For intact skin, permeability measurements were made on the basis of the full skin surface area exposed to the donor solution (2.73 cm^2). Percutaneous absorption for skin treated by microneedles was made on the basis of only the skin area contacting with microneedle arrays.

All results were presented as the average of at least three repeated experiments with its associated standard error from the mean. Statistical analysis was performed by analysis of variance (ANOVA). A probability value of $\alpha=0.05$ was considered statistically significant.

3 Results

3.1 Imaging of microneedle–skin insertion

The microconduits created by microneedles could be easily visualized on the surface of human skin by CLSM. The pattern of dye staining in the stratum corneum was the same as the array of microneedles (Fig. 2).When two spots were chosen and scanned through the *z*-axis (Fig. 3), it was indicated that the fluorescence intensity decreased with the depth. At the depth of 80 μm, the fluorescence intensity was quite weak. Since the fluorescent molecule was applied on the skin in a form of dry film, the diffusion of rhodamine B was negligible. Thus, the penetration depth of rhodamine B could be considered as the depth of microconduits created by microneedle arrays.

Imaging of the dermal side of rat skin indicated that a short period of microneedle insertion had transport macromolecules through the skin *in vivo* (Fig. 4).

3.2 Skin permeability study

The capability of microneedle drug delivery system to enhance skin permeability of calcein was assessed *in vitro*. To avoid the influence of the drug concentration, saturated calcein solution was used as the model drug for *in vitro* percutaneous penetration study. It was demonstrated that the enhancement of transdermal penetration could be increased by 10^4 to 10^5 times compared to that of intact skin, susceptible to delivery parameters of the intradermal delivery system, such as the area and time of insertion (Table 3). This relationship between delivery conditions and the percutaneous permeation would be helpful to improve the dose control in patients.

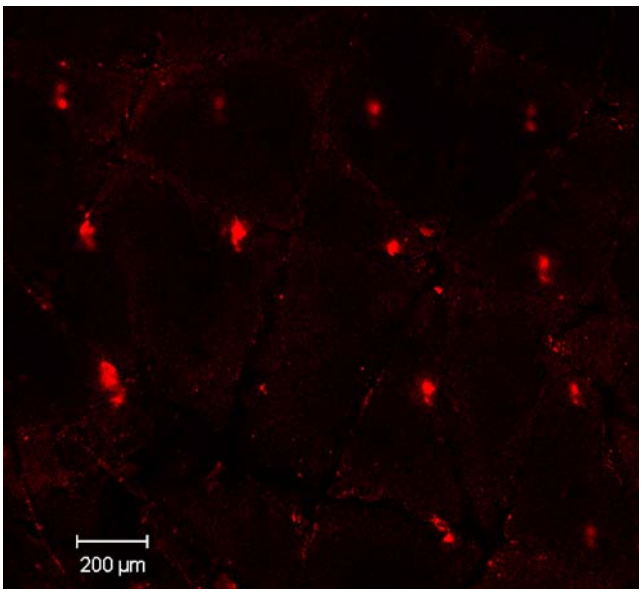

Fig. 2 A fluorescent microscopic image of the outer skin layer after microneedle insertion. The microneedle patch has microneedles of 150 μm long with a density of 484/cm^2

3.2.1 Influence of the insertion area on skin permeation

The influence of insertion area was investigated by means of attaching different amounts of microneedle arrays on the column of the microneedle applicator. The applicator was applied on skin for 10 s. The results indicated that the insertion area played a major role in the transdermal permeability.

As shown in Fig. 5, the larger skin area pierced resulted in significant higher permeation at all points ($p<0.05$). Compared with the transdermal penetration of calcein on intact skin (0.493±0.222 μg at 8 h), the cumulated amount of calcein penetrated was increased with the amount of microneedle wafers. If only one piece of microneedle array was inserted into skin for 10 s, 11.2±3.80 μg of calcein could penetrate the skin after 8 h, but the employment of two, three and four pieces of microneedle arrays led to the significant increase of the cumulated amount of calcein penetrated after 8 hours to 54.6±12.6, 75.0±17.3 and 122±44.9 μg, respectively. It was shown that the cumulated amount of calcein penetrated increased as a linear function of the area with microneedle application ($R^2>0.99$ after 1 h).

3.2.2 Influence of the insertion time on skin permeation

Because of the natural elasticity of skin, the insertion for different periods of time could lead to the difference in the depth of microconduits, which further influenced the transdermal permeation of calcein. Calcein delivered after microneedle treatment for 5 s, 10 s, 20 s, 30 s, 40 s and 60 s are shown in Fig. 6.

It was found that when the insertion time increased from 5 to 40 s, longer insertion time had a positive enhancement effect on the transdermal permeability of calcein. For example, after 8 hours, the cumulated amount of calcein penetrated got to 55.5±12.3, 75.0±17.3, 97.2±11.8, 135.6±19.1 and 150.0±22.7 μg when three pieces of microneedle arrays were applied on skin for 5, 10, 20, 30 and 40 s. However, insertion time longer than 40 s seemed to have little effect on skin permeation. The cumulated amount of calcein penetrated for insertion time as long as 60 s only got to 151.4±54.2 μg after 8 h, with no significant increase from that of 40 s.

3.3 Biological evaluation

The bone marrow micronucleus test in mice employed saline and cyclophosphamide (80.0 mg/kg) as the negative and positive control, respectively. The extraction was

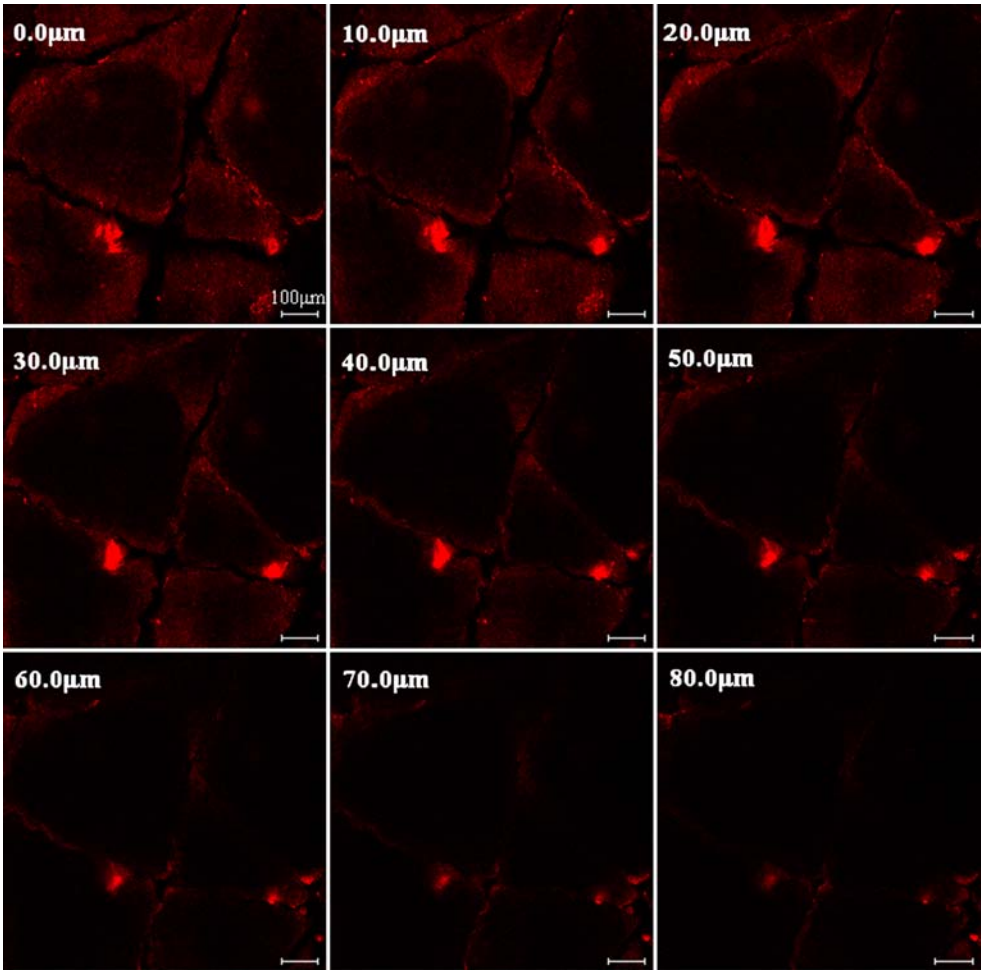

Fig. 3 Penetration of Rhodamine B into human dermatomed skin treated by microneedles as imaged by Confocal Laser Scanning Microscope. Depth 0 indicates the surface of stratum corneum. The microneedle array has a length of 150 μm with 121 needles in an area of 16 mm^2

diluted to half and one quarter of the initial concentration as the moderate and low dose solution. It was shown that the micronucleus rate of the microneedle extraction (1.00± 0.82‰, 0.30±0.67‰ and 1.00±0.94‰ for high, moderate and low dose, respectively) was statistically indistinguishable from that of the negative control (0.60±0.84‰), while for positive control, the micronucleus rate increased to 22.30±5.01‰.

In the Ames bacterial reverse mutation assay, the number of the revertant colonies of the microneedle extraction showed no biologically or statistically significant increases compared to the negative control values, in either the absence or presence of S9. On the other hand, the positive controls of the known mutagens, such as sodium p-(dimethylamino) benzenediazo sulfonate (50 μg/well), sodium azide (2.0 μg/well), 2-nitrofluorene (10 μg/well), significantly increased the number of the revertant colonies.

Cytotoxicity assessment was conducted on BALB/c 3T3. No cytotoxicity was found for the microneedle extraction at such concentration, and the liabilities for microneedle extractions with initial, 1/2, 1/4, 1/8 and 1/16 concentration were 98.2, 95.2, 97.3, 105.2 and 101.4%, respectively. 64 g/L phenol was employed as the positive control, with the livability as low as 19.7%. The result showed that microneedle extraction did not show any cytotoxic reaction using BALB/3T3 cell cultures when incubated for 24 h.

The mammalian cell gene mutation toxicity was investigated using the Chinese Hamster Lung Fibroblast cell cultures. It was found that no biologically or statistically significant increases of mutation data were observed in the presence of S-9 mix for an administration period of either 24 or 48 h.

According to ISO 10993-10:2002 standards, the maximization test was conducted in guinea pigs. The skin sensitization reactions, including erythema and oedema, induced by the microneedle extraction, saline (as the negative control) and methanal (as the positive control) were observed and scored respectively (Table 2).

Skin irritation test was conducted on New Zealand White Rabbits and the allergenic rates and score of the microneedle extraction were 0/3 and 0. Primary skin irritation tests lent support to favorable conclusion, indicating that microneedles caused no irritation reactions by means of their extractable chemicals.

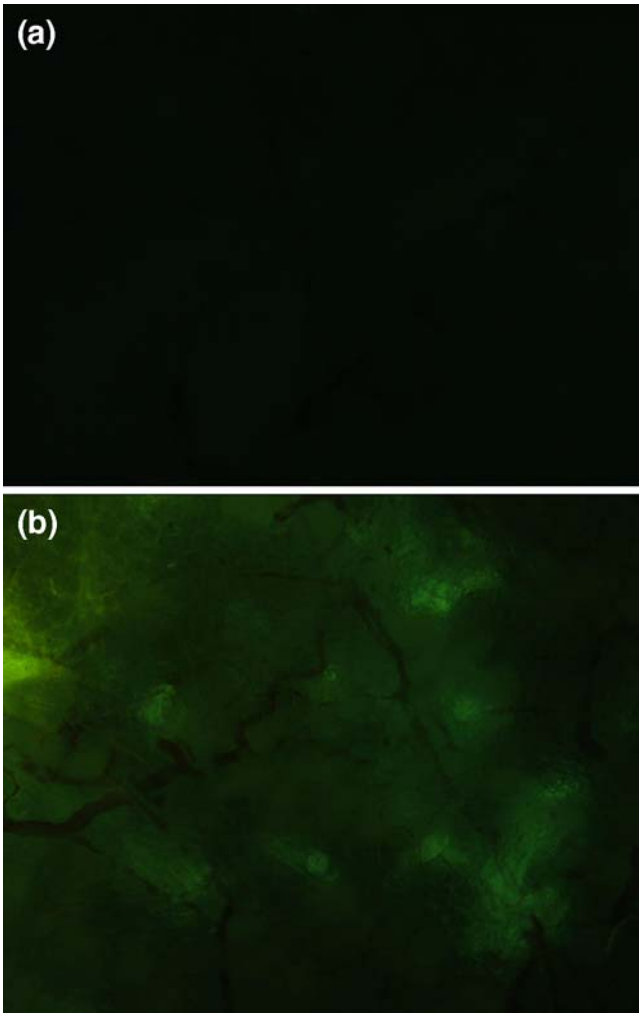

Fig. 4 A comparison of the fluorescent intensity from the dermal side between microneedle treated skin and non-treated skin. The rat full-thickness skin was treated by microneedles for 0 s (**a**) and 10 s (**b**)

4 Discussion

Because of the elasticity of skin tissue, during insertion, some deformation around the insertion site is unavoidable. This deformation significantly reduces the insertion depth of microneedles. According to Martanto et al.'s report (2006), microneedle insertion resulted primarily (approximately 70–90%) in skin indentation. The solutions to the skin deformation include optimizing the geometry of microneedles, increasing the length as well as providing appropriate pressure by the applicators. Several papers have evaluated the influences of microneedle geometry such as the needle length and the sharpness on transdermal permeation efficiency. For example, Haider et al. (2001) suggested an important correlation between application force of microneedles, size of needle and depth of penetration. According to their research, percutaneous penetration would be reduced with the decrease in needle diameter, needle length and inter needle spacing. However,

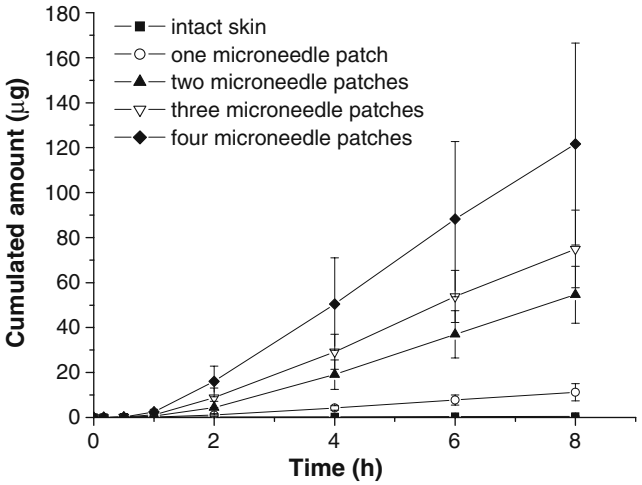

Fig. 5 Comparison of the cumulated amount of calcein penetrated through human skin following the administration of saturated calcein solution onto skins treated by different amounts of microneedle patches. Time 0 indicates the beginning of calcein administration. The microneedle array inserting time was 10 s. The microneedle array used was the patch with microneedles of 150 μm long. Each patch had 121 needles in an area of 4×4 mm^2. (Mean±SD; n=3)

longer microneedles might cause patients' discomfort. Considering the comfort of patients, microneedle arrays with relatively short length were designed in our study. The finished microneedle system had 150 μm long microneedles, which were spaced 400 μm apart, and the self-developed applicator providing an insertion force. To ensure the safety as well as the percutaneous permeation efficiency of silicon microneedles, we recommended octagonal pyramidal microneedles and the installation of the retainer ring onto the applicator; the retainer ring would

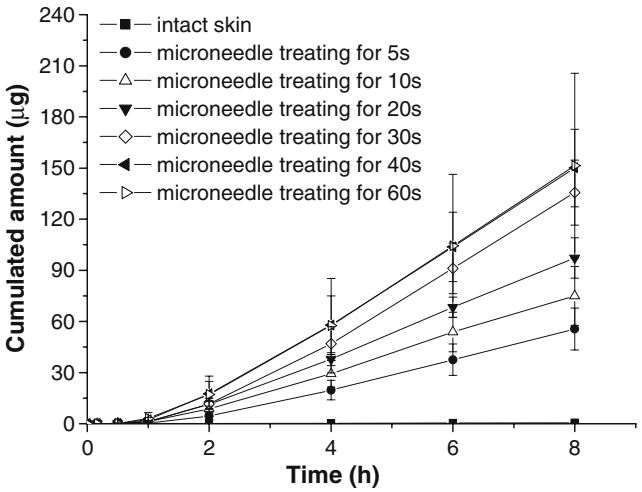

Fig. 6 Comparison of the cumulated amount of calcein penetrated on human skin following the administration of calcein saturated solution onto skins treated by three microneedle patches for different periods of time. Time 0 indicates the beginning of calcein administration. The microneedle array used was the patch with microneedles at the length of 150 μm. Each patch had 121 needles in an area of 4×4 mm^2. (Mean±SD; n=3)

Table 2 Maximization test in guinea pigs

Parameter	Sample number	24 h								48 h								72 h							
		Erythema and eschar					Edema			Erythema and eschar					Edema			Erythema and eschar					Edema		
		0	1	2	3	4	0	1	2	0	1	2	3	4	0	1	2	0	1	2	3	4	0	1	2
Microneedle extract	12	12	0	0	0	0	12	0	0	12	0	0	0	0	12	0	0	12	0	0	0	0	12	0	0
Negative control	6	6	0	0	0	0	6	0	0	6	0	0	0	0	6	0	0	6	0	0	0	0	6	0	0
Positive control	6	0	4	2	0	0	2	4	0	0	0	2	1	3	6	0	0	1	2	3	3	0	6	0	0

Grading of skin reactions

Erythema and eschar formation: no erythema 0, very slight erythema (barely perceptible) 1, well defined erythema 2, moderate to severe erythema 3, severe erythema (beef redness) to eschar formation preventing grading of erythema 4; maximum possible 4

Oedema formation: no oedema 0, very slight oedema (barely perceptible) 1, slight oedema (edges of area well defined by definite raising) 2, moderate oedema (raised approximately 1 mm) 3, severe oedema (raised more than 1 mm and extending beyond area of exposure) 4; maximum possible: 4

help to reduce the impact of skin deformation on the depth of microconduits.

Increasing sharpness improves the percutaneous permeation of microneedles; however, the increased sharpness is sometimes at the expense of the mechanical stiffness. Henry et al. (1998) employed silicon microneedles with quite sharp tips but very thin needle bodies. They mentioned the damage of the top 5–10 μm for microneedles within an array pierced across the stratum corneum of the epidermis sample by the inspection of optical and electron microscopy. In the previous work (Y. Xie et al. 2005), we reported the percutaneous permeation study for microneedles with the geometry similar to those of Chabri et al.'s (2004). The results indicated that 130 μm long microneedles were able to insert into rat skin, but a small portion of microneedle tips would fracture after multiple insertion.

Considering the mechanical properties, our research focused on sharply angled octagonal pyramidal microneedles. The fabrication technology has shown that the height of microneedles could be easily controlled by employing different mask sizes and the etch bath conditions (Xu and Gao 2003; Wilke et al. 2005, 2006; Sasaki et al. 2007). During our permeability studies, the integrity of octagonal pyramidal microneedles was examined before and after each manipulation. After the reuse up to 100 times both *in vitro* and *in vivo*, no fracture or damage of single microneedle was observed. The integrity of these octagonal pyramidal microneedles after administration not only makes repeated use possible, but it also minimizes the risk of irritation caused by the remaining of fragments of broken microneedles in skin.

Compared with those reported (Teo et al. 2006), our microneedle array has a relatively short length of 150 μm. However, this characteristic does not compromise its ability to penetrate the stratum corneum of human dermatomed skin. According to the reports of Henry et al. (1998) and Chabri et al. (2004), a length of 150 μm has been proved to be long enough to increase the permeability of human skin *in vitro*. To improve the penetration efficiency of our microneedles, we fixed 150 μm microneedle arrays onto a column in the applicator, which had a retainer ring (see Fig. 7). The vertical insertion force provided by the applicator, as well as the retainer ring, both facilitated the transdermal permeation of model drug to a great extent, which was indicated by *in vitro* percutaneous studies as well as the microscopy observation.

Under the optical microscope, the microconduits created by these 150 μm microneedles were easily visualized on the surface of human dermatomed skin (Fig. 2). CLSM data indicated that the depth of microconduits was less than 100 μm (Fig. 3), causing no pain to subjects. In comparison, Verbaan et al. (2007) reported that no

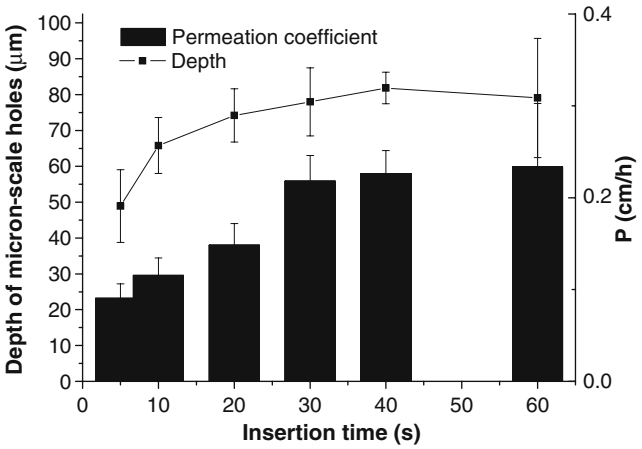

Fig. 7 Comparison of permeability coefficients of calcein on human skin and the depth of microconduits measured from histological frozen section images for samples with different insertion time. The microneedle arrays used were three 150 μm-long microneedle patches, with a density of 484/cm^2. (Mean±SD; $n \geq 4$)

Table 3 Calcein penetrated through human dermatomed skin under different delivering conditions, compared with that on intact skin

Amount of patches	Insertion time (s)	Delay (min)	Js (μg/cm^2/h)	P (cm/h)
1	10	69±22	135±51.7	0.0542±0.0207
2	10	87±28	334±59.6	0.134±0.0238
3	10	59±19	288±47.5	0.115±0.0190
4	10	44±12	252±195	0.101±0.0780
3	5	85±20	226±39	0.0905±0.0157
3	20	54±20	371±58.4	0.148±0.0234
3	30	80±28	545±69.5	0.218±0.0278
3	40	53±19	565±62.7	0.226±0.0251
3	60	67±33	584±172	0.234±0.0690
Intact skin	–	–	0.0202±0.0123	$8.08\times10^{-6}\pm4.92\times10^{-6}$

The microneedles used were 150 μm in length. Each patch has 121 needles in an area of 4×4 mm^2. (Mean±SD; n=3)

appearance of staining dots was observed when dermatomed human skin was pierced with a microneedle array manufactured from commercially available 30 G hypodermal needles with a length of 300 μm. It may be due to the lack of retainer rings and the difference in the geometry of microneedles. The microconduits formation could be further verified by the evidence from *in vivo* and *in vitro* permeation studies. After 150 μm-long microneedle treatment, the exposure of rat abdominal skin to FITC-BSA for 1 h *in vivo* left fluorescent spots on the dermal side of skin (Fig. 4). While calcein hardly penetrated intact human dermatomed skin (600–800 μm), the permeability coefficient of calcein was increased by 10^4 to 10^5 times under a number of different delivery conditions using microneedles (Table 3).

This study explores the efficiency of penetration enhancement under different delivery conditions. As shown in Fig. 5, the insertion area plays an important role. When calcein was applied onto skin for more than 1 h, the cumulated amount of calcein penetrated increased linearly with the insertion area. The results revealed that the enhancement of transdermal penetration depended on the area of microneedle application. The increase could be explained by the formation of more microscale conduits in the skin observed in our results. In clinical practice, this relationship between the insertion area and the skin permeation is believed to be critical to adapt dose levels to individual needs, simply by varying the area with insertion.

Fig. 8 The head of a microneedle intradermal drug delivery system. The microneedle array was fixed onto the supporting column of the applicator, which had a retainer ring

Another parameter taken into account is the insertion time. The increasing of insertion time was expected to alleviate the skin deformation and thus increase the distance of microneedle piercing. The depth measurement of histological section images indicated that the depth of micron-scale holes increased with the prolongation of microneedle insertion, in the scale between 5 to 40 s (Fig. 7), which led to the increase in the cumulated amount of calcein penetrated (Fig. 6). However, as shown in figures, when an insertion time was longer than 40 s, the influence of insertion time to skin permeation began to level off. Both the depth of microconduits and calcein transdermal permeation had no significant difference with that of 40 s insertion time. For a microneedle drug delivery system providing constant pressure, the maximum depth and diameter of micron-scale holes were controlled by the microneedle array Fig. 8. When the insertion time was long enough, for example, 40 s for 150 μm microneedles, skin contraction was overcome by continuous insertion; as a result, the maximum depth and diameter were obtained and further increasing of the insertion time had little influence over the transdermal delivery. This result would help to reduce the inter- and intra-patient variability of transdermal dose delivery caused by the difference in skin elasticity.

This paper is the first report of basic biological safety evaluations on a microneedle device using the ISO safety standards. This assessment criteria leads to a better understanding of the overall biocompatibility of octagonal pyramidal microneedle arrays. In this study, negative results in the safety tests indicate that octagonal pyramidal microneedles should be safe. Further testing would be employed

to secure registration approvals in various markets. However, it should be noted that the microneedle array used in this study was fabricated from single-crystal silicon wafer, which might oxidize on exposure to the air. Coating of SiO_2 on the microneedle surface might improve the biocompatibility of microneedle systems.

5 Conclusion

In this study, we evaluated the percutaneous permeation of drugs under octagonal pyramidal microneedles with the length of 150 μm. Both *in vitro* and *in vivo* microscopy studies support the hypothesis that microconduits were formed in the skin by microneedles; and the microneedles were robust enough to withstand repeated penetration.

In vitro permeation studies demonstrated that the magnitude of permeation improvement could be optimized by regulating the insertion area and insertion time. The permeability increased linearly with the insertion area, and an insertion period longer than 40 s would minimize the effect of the skin deformation around the insertion sites. For device commercialization, the biological evaluation suggested the safety of microneedles for transdermal administration.

In conclusion, our results provide the first systematic evaluation of octagonal pyramidal microneedles as an effective intradermal drug delivery system. The detailed tests *in vivo* of the microneedle intradermal drug delivery system are in progress and will be presented in a different paper.

Acknowledgements We would like to thank Prof. Weidong Hao and his group in the Department of Toxicology of School of Public Health, Peking University, for their support in the biocompatibility evaluation of microneedle arrays; Cheng Zhan (National Institute of Biological Sciences, Peking, China) for Confocal Laser Scanning Microscope (CLSM) imaging of skin samples; the Department of Pathology, Peking University, for their support of frozen tissue sections. The work was partly supported by the Important Direction Program, Chinese Academy of Sciences (No. kjcx2-sw-h12–01).

References

P. Aggarwal, C. R. Johnston, Sens. Actuators B **102**, 226–234 (2004)
F. Chabri, K. Bouris, T. Jones, D. Barrow, A. Hann, C. Allender, K. Brain, J. Birchall, Br. J. Dermatol. **150**, 869–877 (2004)
H. S. Gill, D. Denson and M. R. Prausnitz, *The Preliminary Program for AIChE 2006 Annual Meeting* (San Francisco, USA, 2006)
I. Haider, R. J. Pettis, N. Davison, C. Richard and D. Jeffrey, *Proceedings from the 25th Annual Meeting of the American Society of Biomechanics* (San Diego, CA, 2001)
S. Henry, D. V. McAllister, M. G. Allen, M. R. Prausnitz, J. Pharm. Sci. **87**, 922–925 (1998)
Institute of Laboratory Animal Resources, Commission on Life Sciences, National Research Council, *Guide for the Care and Use of Laboratory Animals* (National Academy Press, Washington, D.C., 1996)
S. Kaushik, A. H. Hord, D. D. Denson, D. V. McAllister, S. Smitra, M. G. Allen, M. R. Prausnitz, Anesth. Analg. **92**, 502–504 (2001)
G. Kotzar, M. Freas, P. Abel, A. Fleischman, S. Roy, C. Zorman, J. M. Moran, J. Melzak, Biomaterials **23**, 2737–2750 (2002)
W. Martanto, S. P. Davis, N. R. Holiday, J. Wang, H. S. Gill, M. R. Prausnitz, Pharm. Res. **21**, 947–952 (2004)
W. Martanto, J. S. Moore, T. Couse, M. R. Prausnitz, J. Control. Release **112**, 351–361 (2006)
D. V. McAllister, M. G. Allen, M. R. Prausnitz, Ann. Rev. Biomed. Eng. **2**, 289–313 (2000)
J. A. Mikszta, J. B. Alarcon, J. M. Brittingham, D. E. Sutter, R. J. Pettis, N. G. Harvey, Nat. Med. **8**, 415–419 (2002)
S. Mitragotri, J. Kost, Adv. Drug Deliv. Rev. **56**, 589–601 (2004)
A. Morrissey, N. Wilke, C. Hilbert and J. O'Brien, *10th International Conference on Electroanalysis, ESEAC04* (Galway, Ireland, 2004)
A. Morrissey, N. Wilke, S. A. Coulman, M. Pearton, A. Anstey, C. Gateley, C. Allender, K. Brain and J. C. Birchall, *The 3rd European Medical and Biological Engineering Conference* (Prague, Czech Republic, 2005)
Organization for Economic Cooperation and Development (OECD), *OECD Guidelines for testing of chemicals, No. 428: Skin Absorption: In vitro Method* (OECD, 2004)
M. R. Prausnitz, Adv. Drug Deliv. Rev. **35**, 61–76 (1999)
M. R. Prausnitz, Adv. Drug Deliv. Rev. **56**, 581–587 (2004)
M. R. Prausnitz, S. Mitragotri, R. Langer, Nat. Rev. Drug Discov. **3**, 115–124 (2004)
M. L. Reed, W-K. Lye, Proceedings of the IEEE **92**, 56–75 (2004)
H. Sasaki, M. Shikida, K. Sato, IEEJ Trans **2**, 340–347 (2007)
A. L. Teo, C. Shearwood, K. C. Ng, J. Lu, S. Moochhala, Mat. Sci. Eng. B **132**, 151–154 (2006)
F. J. Verbaan, S. M. Bal, D. J. van den Berg, W. H. H. Groenink, H. Verpoorten, R. Lüttge, J. A. Bouwstra, J. Control. Release **117**, 238–245 (2007)
A. C. Williams, B. W. Barry, Adv. Drug Deliv. Rev. **56**, 603–618 (2004)
N. Wilke, A. Morrissey, S. Ye and J. O'Brien, EMN04 (Paris, France, 2004), p20–21
N. Wilke, A. Mulcahy, S.-R. Ye, A. Morrissey, Microelectron. J. **36**, 650–656 (2005)
N. Wilke, M. L. Reed, A. Morrissey, J. Micromechanics Microengineering **16**, 808–814 (2006)
N. Wilke, A. Morrissey, J. Micromechanics Microengineering **17**, 238–244 (2007)
Y. Xie, B. Xu, Y. Gao, Nanomedicine: NBM **1**, 184–190 (2005)
B. Xu and Y. Gao, Chinese patent, CN 200310122500 (2003)